Mon. Not. R. Astron. Soc. **000**, 000–000 (0000) Printed 28 November 2007 (MN LATEX style file v2.2)

Constraints on the correlation between QSO luminosity and host halo mass from high-redshift quasar clustering

Martin White[1], Paul Martini[2,3] and J.D. Cohn[4]
[1]*Departments of Physics and Astronomy, University of California, Berkeley, CA 94720*
[2]*Department of Astronomy, The Ohio State University, Columbus, OH 43210*
[3]*Center for Cosmology and Astroparticle Physics, The Ohio State University, Columbus, OH 43210*
[4]*Space Sciences Laboratory, University of California, Berkeley 94720*

28 November 2007

ABSTRACT
Recent measurements of high-redshift QSO clustering from the Sloan Digital Sky Survey indicate that QSOs at $z \sim 4$ have a bias $\langle b \rangle \simeq 14$. We find that this extremely high clustering amplitude, combined with the corresponding space density, constrains the dispersion in the $L-M_h$ relation to be less than 50% at 99% confidence for the most conservative case of a 100% duty cycle. This upper limit to the intrinsic dispersion provides as strong a constraint as current upper limits to the intrinsic dispersion in the local $M_{\rm BH} - \sigma$ relation and the ratio of bolometric to Eddington luminosity of luminous QSOs.

1 INTRODUCTION

It has recently become accepted that quasar activity and black hole growth are an integral part of galaxy evolution, however a detailed understanding of what triggers quasar activity and how they are fueled still eludes us. The leading contender for the identity of luminous, high redshift QSOs is that they are black holes fed by by major mergers of gas-rich galaxies (Carlberg 1990). Recent incarnations of such models (Haiman & Loeb 1998; Cavaliere & Vittorini 2000; Kauffmann & Haehnelt 2000; Wyithe & Loeb 2002; Hopkins et al. 2006) provide a good description of many observed properties of the QSO population.

The situation is particularly interesting at high redshift, where the population of supermassive black holes that powers the QSOs is growing rapidly (see e.g. Fan 2006, for a recent review). To further understand this important phase of black hole and galaxy evolution we would like to build a model in which QSO activity is tied to the evolving cosmic web of dark matter halos. The relationship between QSOs and dark matter halos, their environments and duty cycles, can be constrained via observations of their space density and large-scale clustering (Cole & Kaiser 1989; Haiman & Hui 2001; Martini & Weinberg 2001). These constraints become particularly sensitive if the QSOs inhabit the rarest, most massive halos for which the spatial clustering depends strongly on halo mass (Kaiser 1984; Bardeen et al. 1986; Efstathiou et al. 1988; Cole & Kaiser 1989).

At redshifts $z < 3$ the advent of large optical surveys for QSOs has led to firm constraints on the clustering as a function of luminosity and redshift (Croom et al. 2005; Hennawi et al. 2006; Porciani, Magliocchetti & Norberg 2004; Porciani & Norberg 2006; Myers et al. 2007a,b,c; da Angela et al. 2007). With the Sloan Digital Sky Survey (SDSS) we are now able to measure the clustering of QSOs well even at $z > 3$ (Shen et al. 2007, see also earlier work by Kundic 1997; Stephens et al. 1997). Interestingly, the correlation length of the QSO population increases rapidly with redshift, from $r_0 = 16.90 \pm 1.73$ at $z \simeq 3$ to $r_0 = 24.30 \pm 2.36$ at $z \simeq 4$. Shen et al. (2007) demonstrate that they can fit the observed clustering and space density of $z \sim 4$ QSOs with the model of Martini & Weinberg (2001) provided the $z \sim 4$ QSOs are relatively long lived ($t_Q \sim 160\,$Myr) and inhabit halos more massive than about $5 \times 10^{12}\, h^{-1} M_\odot$. For this calculation Shen et al. (2007) assume that there is a monotonic relationship between instantaneous QSO luminosity and halo mass, with no scatter. The actual relation between instantaneous QSO luminosity and host halo mass is expected to include some scatter. Scatter is expected in several of the relationships linking the QSO luminosity and the host halo mass: the relationship between the host halo mass and galaxy bulge, in the relationship between galaxy bulge and black hole mass, in the relationship between black hole mass and peak luminosity and in the relationship between peak and instantaneous QSO luminosity.

Here we demonstrate that the very high correlation length measured by Shen et al. (2007), when combined with the rapid increase in bias for the most massive halos, strongly constrains the scatter between instantaneous QSO luminosity and halo mass. The essential idea is that any scatter increases the contribution from lower mass (and less highly biased) halos, so that a measurement of large clustering amplitude limits the contribution from lower mass objects. This constraint is as strong as direct, observational constraints at lower redshift on the amount of scatter in the various relationships mentioned above.

We shall work throughout in the ΛCDM framework and adopt the following cosmological parameters: $\Omega_{\rm mat} = 0.25$, $\Omega_\Lambda = 0.75$, $h = 0.72$ and $\sigma_8 = 0.8$. Where appropriate we shall comment on how our results depend on these particular

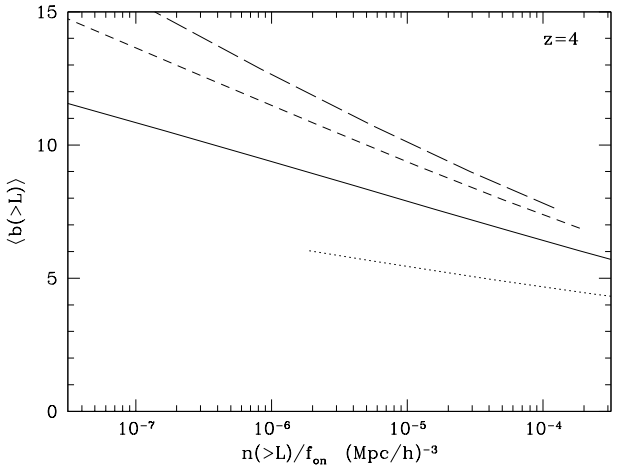

Figure 1. The large-scale bias, $\langle b\rangle$, vs. the space density for all QSOs at $z = 4$ above a luminosity threshold assuming a log-normal relationship between instantaneous QSO luminosity and halo mass with dispersion $\sigma = 0.1$ (long dashed), 0.5 (dashed), 1 (solid) and 2 (dotted). The case $\sigma = 0$ (not shown) is almost indistinguishable from $\sigma = 0.1$. In each case the lines run from $M_t = 10^{12}$ to $10^{14.5}\,h^{-1}M_\odot$.

choices. The next section outlines our formalism and applies it to the data of Shen et al. (2007), while §3 interprets our results and discusses future observations.

2 FORMALISM AND APPLICATION TO HIGH-REDSHIFT QSOS

2.1 The clustering and abundance of QSOs

We will focus our attention on the space density and large-scale bias of QSOs, as these are the easiest to interpret, observationally measurable properties of the population. If the mean number of QSOs in a halo of mass M_h is $N(M_h)$ then their number density and large-scale bias are

$$\bar{n} = \int dM_h\, \frac{dn_h}{dM_h} N(M_h) \quad (1)$$

$$\langle b\rangle = \bar{n}^{-1} \int dM_h\, \frac{dn_h}{dM_h} b_h(M_h) N(M_h) \quad (2)$$

where dn_h/dM_h is the (comoving) number density of halos per mass interval and $b_h(M_h)$ is the bias associated with halos of that mass. For dn_h/dM_h we use the fitting function from Sheth & Tormen (1999). The large-scale bias is slightly more problematic, as our results depend upon massive halos being biased and different fits to $b_h(M_h)$ from simulations have appeared in the literature. Sheth & Tormen (1999) derived the bias appropriate to their mass function fit using the peak background split. A slightly higher bias at fixed mass comes from assuming ellipsoidal collapse (Sheth, Mo & Tormen 1999). The largest bias for halos of a given mass is given by the bias of the Press & Schechter (1974) mass function, which is very similar to the fit of Jing (1998) for the masses of interest. These two forms give biases 30% larger, in the mass and redshift range of interest, than the lowest fit (of Sheth & Tormen 1999). The fit of Tinker et al. (2005) lies between that of Sheth, Mo & Tormen (1999) and Sheth & Tormen (1999). For mass-thresholded samples of dark matter halos in a large N-body simulation[1], we found the Press & Schechter (1974) and Sheth & Tormen (1999) forms bracketed the halo correlation function so this should represent the level of current uncertainty. As it provides the most conservative estimate of the maximum allowed scatter, and the numerical data lay closer to the form of Press & Schechter (1974), we adopt this as our fiducial bias. However, we caution that the statistics in the simulation are poor and we also illustrate the effect of choosing the Sheth & Tormen (1999) form below. In several recent simulations at other redshifts and masses the Press & Schechter (1974) form appears to be a worse fit (Sheth & Tormen 1999; Sheth, Mo & Tormen 1999; Seljak & Warren 2004; Tinker et al. 2005), but unfortunately there are few direct N-body calibrations of $b_h(M)$ at the number densities and redshifts of interest to us. This challenging numerical problem deserves further investigation.

To interpret the large-scale clustering measurements of Shen et al. (2007) we then must specify $N(M_h)$. We wish to choose as simple a model as possible to illustrate the effect of scatter on the $\langle b\rangle - \bar{n}$ relation, so we assume that the probability that a QSO is seen with instantaneous luminosity L is log-normally distributed[2] around a central value $L_0(M_h)$ with a width σ. If we assume that at most a fraction $f_{\rm on}$ of halos host active QSOs at any epoch, the mean number of QSOs above a luminosity threshold $L_{\rm min}$ is

$$N(M_h) = \frac{f_{\rm on}}{2}\,{\rm erfc}\,\left[\frac{\ln M_t/M_h}{\sqrt{2}\sigma}\right] \quad (3)$$

where $L_0(M_t) \equiv L_{\rm min}$. Figure 1 shows $\langle b(>L)\rangle$ vs. $\bar{n}(>L)/f_{\rm on}$ for a range of M_t and σ. The larger the dispersion the lower the bias at fixed space density, as a larger fraction of the QSOs are hosted in lower mass halos. Similarly, a decrease in $f_{\rm on}$ must be compensated by a decrease in M_t to hold $\bar{n}$ fixed, again leading to a lower $\langle b\rangle$. In our assumed cosmology the Universe is $t_U \simeq 1.6$Gyr old at $z = 4$. If we assume $L_{\rm bol}/L_{\rm edd} = 0.25$ (e.g. Kollmeier et al. 2006) then the e-folding time is $\simeq 0.1\,t_U$, so $f_{\rm on} \sim \mathcal{O}(1)$ is not unexpected. While the inferred lifetimes are then weakly in conflict with the upper range of observational constraints ($10^6 - 10^8$ years; Martini 2004), these constraints largely stem from lower-redshift QSOs.

Our model is not the most general one describing how QSOs inhabit dark matter halos. In particular there is no reason in principle why halos could not host more than one QSO (i.e. $f_{\rm on} > 1$). To constrain the functional form of $N(M_h)$ would require modeling both the large- and small-scale clustering, and additional assumptions about the statistics of QSOs in halos. This is beyond the scope of this paper, so we merely note that the mass function is very steeply falling in the range of halo masses that are of interest. Our statistics are thus dominated by the lowest mass

[1] The simulation evolved 1024^3 particles in a $1\,h^{-1}$Gpc box using the *TreePM* code described in White (2002). See Heitmann et al. (2007) for a recent comparison with other N-body codes.

[2] We use natural logarithms throughout so that σ can be interpreted as a fractional scatter. The log-base-10 based σ would be $\ln(10) \simeq 2.3$ times smaller.

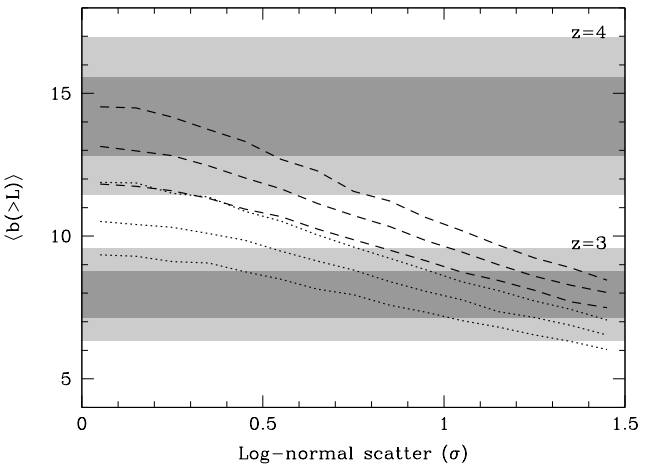

Figure 2. The large-scale bias, $\langle b\rangle$, vs. log-normal dispersion, σ, for all QSOs brighter than a given $L_{\rm min}$ chosen such that $\bar{n} = 5.6\times10^{-7}\,h^3{\rm Mpc}^{-3}$ (lower, dotted lines) or $2\times10^{-7}\,h^3{\rm Mpc}^{-3}$ (upper, dashed lines). The shaded bands indicate the ±1 and 2σ range of bias measured by Shen et al. (2007), as described in the text. For each triple of lines the upper line assumes $f_{\rm on}$ of Eq. (3) is unity while the lower lines assume $f_{\rm on} = 0.3$ and 0.1.

halos in our sample. In particular the number density is approximately linear in $N(M_t)$. To increase $\bar{n}$ significantly above that for our model would require almost every halo of mass M_t to host more than one high luminosity QSO which would lead to an unacceptably high close pair fraction. For example if every halo hosted 2 QSOs the integrated correlation function within the halo virial radius would be $\bar{\xi}\sim n_h^{-1}r_h^{-3}$. Given the extreme rarity of these halos, this would be in conflict with observations (Hennawi et al. 2006; Myers et al. 2007b, see e.g. Fig. 17 in Hopkins et al. 2007b).

At this point it is also easy to see how a change in cosmological parameters affects $\langle b\rangle-\bar{n}$. For example, if we raise σ_8, halos of a fixed mass correspond to less rare peaks. These halos are therefore slightly less biased and significantly more numerous. To hold $\bar{n}$ fixed we would need to increase M_t. To hold the bias fixed requires that we increase M_t yet further and therefore to match both the $\langle b\rangle$ and $\bar{n}$ the duty cycle must increase. For $\bar{n}\simeq10^{-7}h^3{\rm Mpc}^{-3}$, a 10% increase in σ_8 leads to a 4% decrease in $\langle b\rangle$, which is insignificant for our purposes. In general, for a power-law power spectrum with index $n_{\rm eff}$, the fractional change in number density at fixed bias is $6/(3+n_{\rm eff})$ times the fractional change in σ_8. Small changes in the other cosmological parameters have even smaller effects.

2.2 Comparison with observations

This formalism allows us to use the observations of high-z QSO clustering from Shen et al. (2007) to constrain σ and $f_{\rm on}$ in our model. To do so we need to estimate the large-scale bias, $\langle b\rangle$, from the measurements provided in Shen et al. (2007) and this requires making several assumptions.

First we must convert from the clustering quoted by Shen et al. (2007) to large-scale bias. There are several ways to do this, and we have chosen to use the amplitude of their fits to r^{-2} power-laws over the range $5<r<20\,h^{-1}$Mpc. At lower z the bias is relatively constant over this range and the slope of the dark matter correlation function is close to -2, so converting the fit into a measurement of $\langle b\rangle$ is straightforward. However at $z>3$ the QSOs are hosted by increasingly rare halos, whose bias is becoming more scale dependent. Using the mass and halo catalogs from the N-body simulation described previously we find that the mass correlation function is shallower than r^{-2} below $\mathcal{O}(10\,h^{-1}{\rm Mpc})$ but the halo correlation function is still quite close to r^{-2} down to $5\,h^{-1}$Mpc. We therefore convert from r_0 to $\langle b\rangle$ by matching

$$\xi_{qq}=\left(\frac{r_0}{r}\right)^2=\langle b\rangle^2\xi_{\rm dm}(r) \tag{4}$$

at $r=20\,h^{-1}$Mpc, where the bias is close to constant. (This is also the scale where we compared the simulations to the Press & Schechter (1974) fitting form to obtain the bias.) For convenience we use the non-linear power spectrum of Smith et al. (2003) when computing $\xi_{\rm dm}$, but we checked that this agrees well with the results of the N-body simulation on the scales of interest and the correction for non-linearity is relatively small.

The clustering measurements of Shen et al. (2007) are averaged over bins in redshift, over which the bias and mass correlations are evolving strongly. Fortuitously, the effects approximately cancel, leading to a slow evolution in ξ_{qq}. We estimate the effects of clustering evolution on our constant-time constraints by considering 3 models for the evolution: passive evolution (which for massive, rare halos corresponds almost to ξ_{qq} =constant), constant bias and constant halo mass. Each model predicts $\xi_{qq}(r,z)$ from which we can compute the average value measured by Shen et al. (2007) as

$$\langle\xi(r)\rangle\equiv\frac{\int dz\ (dN/dz)^2(H/\chi^2)\xi(r,z)}{\int dz\ (dN/dz)^2(H/\chi^2)} \tag{5}$$

where dN/dz is the redshift distribution, H is the Hubble parameter at redshift z and χ is the comoving angular diameter distance to redshift z. Using dN/dz from Table 1 of Shen et al. (2007) in the two bins $2.9<z<3.5$ and $z>3.5$ we find that for the passive evolution model the correlation length inferred from $\langle\xi\rangle$ is within 1% of that inferred from $\xi(z=3)$ and $\xi(z=4)$ respectively. For the constant halo mass case $\xi(z)$ increases with z, but the inferred r_0 is still within 5% of the constant z value for both samples. For the constant bias case, $\xi(z)$ decreases with z, but the inferred r_0 is within 4% of the constant z value for both samples. Since the quoted errors on r_0 are larger than this, we shall interpret the quoted correlation lengths as measurements at $z=3$ and $z=4$ respectively.

Assuming $\xi_{qq}=(r_0/r)^2$, Shen et al. (2007) quote $r_0=(16.90\pm1.73)\,h^{-1}$Mpc for their "good" sample with $2.9<z<3.5$. Using the dark matter correlation function for our cosmology at $z=3$ this corresponds to $\langle b\rangle=7.9\pm0.8$. The quoted space density is $\bar{n}=5.6\times10^{-7}\,h^3{\rm Mpc}^{-3}$. If we use the 'all' sample both r_0 and hence $\langle b\rangle$ are 14% lower. We will find that this point is relatively unconstraining for either choice.

At $z=4$ the best fit is $r_0=(24.30\pm2.36)\,h^{-1}$Mpc, again using the "good" sample, corresponding to $\langle b\rangle=14.2\pm1.4$, and $\bar{n}=10^{-7}\,h^3{\rm Mpc}^{-3}$. The other clustering fits provided by Shen et al. (2007) are discussed below. Note however, as pointed out by Shen et al. (2007), this

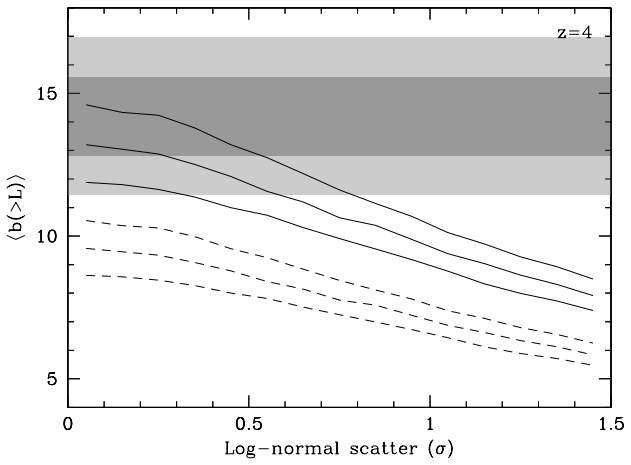

Figure 3. The same range of measured bias for $z = 4$ as shown in Fig. 2, but now for two different analytic fits to the theoretical bias. The Press-Schechter (top, solid) bias fit is as before, the Sheth-Tormen (bottom, dashed) is shown below. Again the shaded bands indicate the ± 1 and 2σ range of bias for $z = 4$ measured by Shen et al. (2007), as described in the text. For each triple of lines the upper line assumes $f_{\rm on}$ of Eq. (3) is unity while the lower lines assume $f_{\rm on} = 0.3$ and 0.1. If the Sheth-Tormen bias is used, there is no overlap within the 2σ range of the clustering measurement.

space density is actually an underestimate of the true space density because the Richards et al. (2006) parameterization of the LF underestimates the measured space density from $z \sim 3 \to 4$ (see Figure 20 of Richards et al. 2006). At $z \simeq 4$ this underestimate is approximately a factor of two and we therefore use $\bar{n} = 2 \times 10^{-7}\, h^3 {\rm Mpc}^{-3}$. The higher space density leads to a smaller predicted $\langle b \rangle$, requiring smaller dispersion σ between luminosity and halo mass to fit the observed clustering (i.e. this provides a more stringent constraint).

In Fig. 2 we show $\langle b(>L) \rangle$ as a function of log-normal scatter, σ, at fixed $\bar{n}$ for $f_{\rm on} = 1$, 0.3 and 0.1. The 68% and 95% confidence ranges in $\langle b \rangle$ (above) are also shown. As can be seen, in order to get the large $\langle b \rangle$ seen by Shen et al. (2007), the scatter at $z \simeq 4$ has to be less than 80% and the fraction of halos containing quasars, $f_{\rm on}$, must be larger than $\sim 10\%$.

The constraints will change if different fits to the clustering measurements, different fits for b_h, or different number densities are used. As the constraints are coming from $z = 4$, we focus on this case. Shen et al. (2007) gives 4 fits to power-law correlation functions, for "all" or "good" QSO's, with fixed power law $(r_0/r)^2$ or varying power law. The fiducial calculation above was for the "good" QSOs sample fit to $(r_0/r)^2$, which has a $\chi^2/{\rm dof} = 0.32$. The other combinations give: (sample, power-law index, χ^2, $\delta b/b$)= ("all", 2.00, 0.52, -15%), ("good", 2.14, 0.32, +6%), ("all", 2.28, 0.50, -6%). The central value in Fig. 2 then just moves up and down by the shift in bias (the error bars do change slightly in width). Our example in Fig. 2 is one of the best χ^2 cases but also gives a high bias (and thus is very constraining).

As mentioned previously, our fiducial b_h was chosen to give the least stringent constraint. The functional forms of Sheth & Tormen (1999); Sheth, Mo & Tormen (1999); Seljak & Warren (2004), and Tinker et al. (2005) predict lower b_h at fixed M_h and hence tighter constraints on σ and $f_{\rm on}$. We illustrate the range in Figure 3, which compares the results using our fiducial bias to that of Sheth & Tormen (1999). The bias from N-body simulations, where they are available, tends to lie between those of Sheth & Tormen (1999) and Sheth, Mo & Tormen (1999) which differ from each other by $5 - 10\%$ in the mass and redshift range of interest (see also Seljak & Warren 2004; Tinker et al. 2005). Neither the Sheth-Tormen or Sheth-Mo-Tormen biases are able to fit the measured bias and number density.

The most unconstraining estimate would be to use the lower amplitude of clustering, e.g. the "all" sample, at $z = 4$. We did not choose this because there are a number of systematics which could lower the measured clustering amplitude and the "all" sample has a worse χ^2. But if taken in conjunction with the (most conservative) Press-Schechter bias and the highest allowed number density, the limit can be weakened to allow $\sigma = 1$ at 95% confidence for $f_{\rm on} = 0.1$. It is also possible that QSOs may inhabit a special subclass of halos for which the bias is larger than the average for that mass. For instance there are indications that halo history affects clustering in some cases (Wechsler et al 2006; Wetzel et al. 2007; Gao & White 2007; Croton, Gao & White 2007; Jing, Suto & Mo 2007). For the very rare and highly biased halos hosting QSOs at $z \simeq 4$ this effect may be large enough to weaken our constraint. Unfortunately the bias of the relevant objects has not yet been measured in simulations.

3 DISCUSSION

It appears that the most luminous, highest redshift QSOs have instantaneous luminosities which are well correlated with their host halo masses. The already strong constraint shown here should be improved by measurements of high-redshift QSO clustering with yet larger samples. New observations will broadly improve the constraint in two ways: through wider area observations to identify a larger number of QSOs similar in redshift to the SDSS sample, and through deeper observations over the same area. Deeper observations will identify slightly fainter QSOs at all redshifts and may provide a sufficient sample to measure the clustering amplitude at even higher redshift than $z \sim 4$, where we expect the bias to be even larger. Going wider in area will decrease the fractional error on $\langle b \rangle$ for high-redshift QSOs. As these measurements of high-redshift QSO bias will remain Poisson limited, the fractional error on $\langle b \rangle$ will scale as $1/N_{\rm qso}$ for a survey of $N_{\rm qso}$ QSOs. Going deeper to measure luminous QSOs at yet higher redshifts is also expected to be useful, as the data indicate strong evolution in the clustering amplitude with redshift.

Figure 4 illustrates how $\langle b \rangle$ increases with redshift for three values of the scatter between QSO luminosity and host halo mass assuming $f_{\rm on} = 1$. At each redshift $\langle b \rangle$ was calculated to match the QSO space density evolution parametrized by Richards et al. (2006), although converted to our cosmological parameters[3]. The steepest relation be-

[3] For simplicity we did not correct the Richards et al. (2006) LF parameterization to match their binned LF here. The space

tween $\langle b \rangle$ and redshift is for the case of the smallest scatter. If $f_{\rm on} = 1$ and the scatter is minimal, the relative value of $\langle b \rangle$ for different values of the dispersion is a good measure of the fractional uncertainty in $\langle b \rangle$ required to improve on our constraint. These ratios demonstrate that the most effective constraint from clustering arises from the lowest redshift at which $f_{\rm on} = 1$ and minimal scatter is a reasonable approximation. For example, the ratio of $\langle b \rangle(\sigma = 0.1)$ to $\langle b \rangle(\sigma = 1.0)$ increases by less than 10% from $z = 4$ to $z = 5$, while the $N_{\rm qso}$ above the SDSS flux limit drops by approximately an order of magnitude. Therefore while the clustering amplitude increases, the decline in $N_{\rm qso}$ for a flux-limited, high-redshift survey more than offsets this gain. By contrast, color selection of just very high-redshift (e.g. $z > 5$) QSOs could produce a substantial improvement for a given total number of spectra.

The immediate prospect for improvement in this constraint is completion of the SDSS observations beyond the 4000 square degrees employed by Shen et al. (2007). These observations will simply increase $N_{\rm qso}$ and the error bars should scale as $N_{\rm qso}^{-1}$. On a somewhat longer timescale, the proposed Baryon Oscillation Spectroscopic Survey (BOSS[4]) should approximately double the number of $z > 3.5$ QSOs, although it will mostly achieve this by going deeper. Provided $f_{\rm on} = 1$ and small scatter are still reasonable approximations to this slightly fainter population (that will still be well above the break in the QSO LF), BOSS' factor of two improvement in sample size should decrease the error bars by approximately a factor of two and produce a powerful improvement in the constraint. For example, if the measured bias stayed fixed and the errorbars decreased by a factor of two, the upper limit on the observed scatter would improve to less than 0.5 (i.e. 0.2 dex) for $f_{\rm on} = 1$. There are also upcoming photometric surveys that go even wider in area and deeper: Pan-STARRS[5], the Dark Energy Survey (DES[6]), and the Large Synoptic Survey Telescope (LSST[7]). While these surveys do not include a dedicated plan for spectroscopic observations of QSOs, they will provide the necessary candidate database of these extremely rare objects for spectroscopy.

On the theoretical side, the calculations presented here could also be improved. Better modeling could allow us to use a wider range of scales. As large-scale, high-resolution simulations become increasingly feasible, it will become possible to precisely measure both the bias of all halos and the bias as a function of halo history. The scatter between these various relationships can also be measured in self-consistent numerical simulations of merger-driven black hole growth. Hopkins et al. (2007b) presented a recent analysis of the observed and simulated scatter between black hole mass and various host (bulge) galaxy properties (σ, host galaxy mass, effective radius) at lower redshifts than we are considering here. They find that the intrinsic scatter is generally lower than the observed (upper limit) and as small as ~ 0.2 dex for combinations that produce a fundamental plane for black holes. However, they also note that the strong correlation of black hole mass with bulge properties implies that the connection to halo mass is only indirect and dominated by the evolution in the typical gas fractions. Measurement of the evolution of these quantities in full cosmological simulations (e.g. Di Matteo et al. 2007) could provide measurements of the expected scatter at the very high redshifts where QSOs are observed to be so strongly biased.

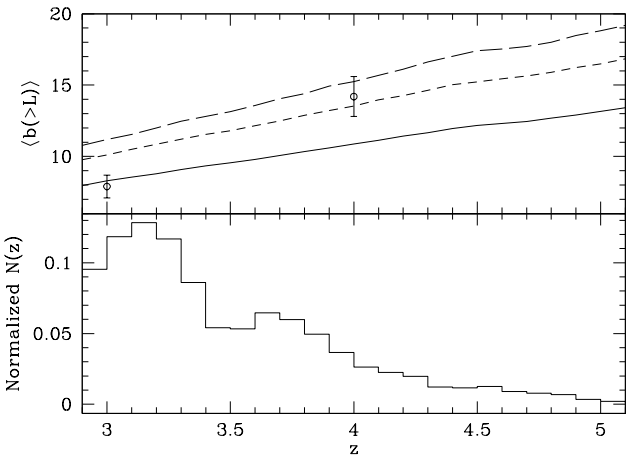

Figure 4. (*Top*) The large-scale bias, $\langle b \rangle$, vs. redshift of halos that match the integrated QSO space density from Richards et al. (2006) for $f_{\rm on} = 1$ and dispersion $\sigma = 0.1$ (long dashed), 0.5 (dashed), 1 (solid) as in Figure 1. Our bias estimates derived from the (Shen et al. 2007) estimates are also shown. (*Bottom*) Normalized number of QSOs per redshift bin from Shen et al. (2007). The rapid decrease in SDSS QSOs with redshift indicates that purely flux-limited surveys at $z > 3$ can not place as strong a constraint on σ at yet higher redshifts, even though those QSOs are more strongly biased.

Regardless of these future prospects, the strength of the present constraint on scatter in a monotonic relation between QSO luminosity and halo mass is already surprising. As noted in the introduction, we expect scatter to be present because we expect scatter in at least four relationships that combine to determine the instantaneous luminosity of a QSO in a halo of a given mass: the relationship between instantaneous luminosity and peak luminosity; the relationship between peak luminosity and black hole mass; the relationship between black hole mass and bulge properties; and the relationship between bulge and halo mass. These expectations arise from the observed scatter in these individual relations at lower redshifts–intriguingly, in all cases the observed scatter only sets an upper limit on the intrinsic scatter.

For the relation between black hole mass and bulge velocity dispersion known as the $M_{\rm BH}-\sigma$ relation (Ferrarese & Merritt 2000; Gebhardt et al. 2000), Tremaine et al. (2002) showed that the intrinsic dispersion is no larger than 0.25–0.3 dex (or $\sigma = 0.58 - 0.70$ in our natural log notation). Ferrarese (2002) explored the relation between $M_{\rm BH} - M_h$ by using rotation curve data and argued that the dispersion between black hole and halo mass could be even less than the $M_{\rm BH} - \sigma$ dispersion, although she notes that the uncertainty in the transformation between circular velocity

density has therefore been slightly underestimated from $z = 3 \rightarrow 4$ and consequently the predicted bias is slightly higher.

[4] http://cosmology.lbl.gov/BOSS
[5] http://pan-starrs.ifa.hawaii.edu
[6] http://www.darkenergysurvey.org
[7] http://www.lsst.org

and halo mass is not well characterized. Finally, Kollmeier et al. (2006) measured the distribution in Eddington ratio, $L_{\rm bol}/L_{\rm Edd}$, for a sample of $z = 0.3 - 4$ QSOs and find the distribution is well described as log-normal with a peak at 0.25 and a dispersion of 0.3 dex. As this observed dispersion must account for the uncertainty in the mass estimator and bolometric correction in addition to $L_{\rm bol}/L_{\rm Edd}$, this measurement also sets an upper limit to the intrinsic dispersion in $L_{\rm bol}/L_{\rm Edd}$.

In addition to the small scatter in $L-M_h$, the data also suggest that the duty cycle is approximately unity. This may be less surprising, given their extremely high luminosities and masses of their supermassive black holes. If QSOs are limited to accreting at no more than the Eddington rate, the luminosities of $z > 6$ QSOs imply that their central, supermassive black holes already exceeded $M_{\rm BH} \sim 10^9 M_\odot$ when the Universe was less than 1 Gyr old (Fan et al. 2001). Subsequent near-infrared spectroscopy provides further evidence that their central black holes are indeed this massive (Barth et al. 2003; Jiang et al. 2007). To create such massive black holes at early times requires $f_{\rm on} \sim 1$, modulo the uncertainty in the initial seed mass. Together, these strong constraints on the duty cycle and scatter in $L-M_h$ for high-redshift QSOs provide important new information on how supermassive black holes and their host halos grew at early times.

We thank Yue Shen and Cris Porciani for helpful comments on an earlier draft of this paper. The simulations used in this paper were analyzed at the National Energy Research Scientific Computing Center. We thank CCAPP at The Ohio State University and the participants in the quasar mini-workshop for a stimulating meeting. JDC and MW also are grateful to CCAPP for hosting them for an extended visit. MW is supported by NASA.

REFERENCES

da Angela J., et al., 2007, preprint [astro-ph/0612401]
Bardeen, J., Bond, J.R., Kaiser, N., & Szalay, A.S. 1986, ApJ, 304, 15
Barth, A.J., Martini, P., Nelson, C.H. Ho, L.C., 2003, ApJ, 594, L94
Carlberg R., 1990, ApJ, 350, 505
Cavaliere, A., & Vittorini, V., 2000, ApJ, 543, 599
Cole S., Kaiser N., 1989, MNRAS, 237, 1127
Croom S.M., et al., 2005, MNRAS, 356, 415
Croton, D. J., Gao, L., White, S. D. M, 2007, MNRAS, 374, 1303
Efstathiou G., Frenk C.S., White S.D.M., Davis M., 1988, MNRAS, 235, 715
Fan, X. et al. 2001, AJ, 122, 2833
Fan, X., 2006, NewAR, 50, 655
Ferrarese, L. & Merritt, D. 2000, ApJ, 539, L9
Ferrarese, L. 2002, ApJ, 578, 90
Gao, L, White, S.D.M., 2007, MNRASL, 377, 5
Gebhardt, K. et al. 2000, AJ, 119, 1157
Haiman Z., Loeb, A. 1998, ApJ, 503, 505
Haiman Z., Hui L., 2001, ApJ, 547, 27
Heitmann K., et al., 2007, Computational Science and Discovery, in press [arxiv/0706.1270]
Hennawi J.F., et al., 2006, AJ, 131, 1
Hopkins, P.F., Hernquist, L.E., Cox, T.J., Robertson, B., Krause, E., 2007a, ApJ to appear, preprint [astro-ph/0701351]
Hopkins P.F., Hernquist L., Cox T.J., Keres D., 2007b, ApJ, to appear [arXiv:0706.1243]
Hopkins, P.F. et al., 2006, ApJS, 163, 1
Jiang, L. et al. 2007, AJ, 134, 1150
Jing Y.P., 1998, ApJ, 503, L9
Jing, Y. P., Suto, Y., Mo, H. J., 2007, ApJ, 657, 664
Kaiser, N. 1984, ApJ, 284, L9
Kauffmann, G., Haenelt, M., MNRAS, 2000, 311, 576
Kollmeier, J.A. et al. 2006, ApJ, 648, 128
Kundic T., 1997, ApJ, 482, 631
Martini P., Weinberg D.H., 2001, ApJ, 547, 12
Martini, P. 2004, in Coevolution of Black Holes and Galaxies, ed. L. C. Ho (Cambridge: Cambridge Univ. Press), 235
Di Matteo, T., Colberg,J., Springel, V., Hernquist, L., Sijacki, D., 2007, preprint[arXiv:0705.2269]
Myers A.D., Brunner R.J., Nichol R.C., Richards G.T., Schneider D.P., Bahcall N.A., 2007a, ApJ, 658, 85
Myers A.D., Brunner R.J., Nichol R.C., Richards G.T., Schneider D.P., Bahcall N.A., 2007a, ApJ, 658, 99
Myers, A.D., Richards, G.T., Brunner, R.J., Schneider, D.B., Strand, N.E., Hall, P.B., Blomquist, J.A., York, D.G., 2007c, preprint[arxiv:0709.3474]
Porciani C., Magliocchetti M., Norberg P., 2004, MNRAS, 355, 1010
Porciani C., Norberg P., 2006, MNRAS, 371, 1824
Press W.H., Schechter P., 1974, ApJ, 187, 425
Richards, G.T. et al. 2006, AJ, 131, 2766
Seljak U., Warren M.S., 2004, MNRAS, 355, 129
Shen Y., et al., 2007, preprint [astro-ph/0702214]
Sheth R., Tormen G., 1999, MNRAS, 308, 119
Sheth R., Mo H.-J., Tormen G., 2001, MNRAS, 323, 1
Smith R.E., Peacock J.A., Jenkins A., White S.D.M., Frenk C.S., Pearce F.R., Thomas P.A., Efstathiou G., Couchman H.M.P., 2003, MNRAS, 341, 1311
Stephens A.W., Schneider D.P., Schmidt M., Gunn J.E., Weinberg D.H., 1997, AJ, 114, 41
Tinker, J.L., Weinberg, D.H., Zheng, Z., Zehavi, I., 2005, ApJ, 631, 41
Tremaine, S. et al. 2002, ApJ, 574, 740
Wechsler, R.H., Zentner, A.R., Bullock, J.S. Kravtsov, A.V., Allgood, B., 2006, ApJ, 652, 71
Wetzel A., Cohn J.D., White M., Holz D.E., Warren M.S., 2007, ApJ, 656, 139
White M., 2002, ApJS, 579, 16
Wyithe, J.S.B., Loeb, A., 2002, ApJ, 581, 886